

# A low escape fraction of ionizing photons of $L > L^*$ Lyman break galaxies at $z=3.3$

K. Boutsia<sup>1</sup>, A. Grazian<sup>1</sup>, E. Giallongo<sup>1</sup>, A. Fontana<sup>1</sup>, L. Pentericci<sup>1</sup>, M. Castellano<sup>1</sup>, G. Zamorani<sup>2</sup>, M. Mignoli<sup>2</sup>, E. Vanzella<sup>3</sup>, F. Fiore<sup>1</sup>, S. J. Lilly<sup>4</sup>, S. Gallozzi<sup>1</sup>, V. Testa<sup>1</sup>, D. Paris<sup>1</sup>, P. Santini<sup>1</sup>

<sup>1</sup>*INAF - Osservatorio Astronomico di Roma, Via Frascati 33, I-00040, Monteporzio, Italy*

<sup>2</sup>*INAF - Osservatorio Astronomico di Bologna, Via Ranzani 1, I-40127, Bologna, Italy*

<sup>3</sup>*INAF - Osservatorio Astronomico di Trieste, Via G.B. Tiepolo 11, I-34131, Trieste, Italy*

<sup>4</sup>*Institute of Astronomy, ETH Zürich, CH-8093, Zürich, Switzerland*

## ABSTRACT

We present an upper limit for the relative escape fraction ( $f_{esc}^{rel}$ ) of ionizing radiation at  $z \sim 3.3$  using a sample of 11 Lyman Break Galaxies (LBGs) with deep imaging in the U band obtained with the Large Binocular Camera, mounted on the prime focus of the Large Binocular Telescope. We selected 11 LBGs with secure redshift in the range  $3.27 < z < 3.35$ , from 3 independent fields. We stacked the images of our sources in the R and U band, which correspond to an effective rest-frame wavelength of  $1500\text{\AA}$  and  $900\text{\AA}$  respectively, obtaining a limit in the U band image of  $\geq 30.7(\text{AB})\text{mag}$  at  $1\sigma$ . We derive a  $1\sigma$  upper limit of  $f_{esc}^{rel} \sim 5\%$ , which is one of the lowest values found in the literature so far at  $z \sim 3.3$ . Assuming that the upper limit for the escape fraction that we derived from our sample holds for all galaxies at this redshift, the hydrogen ionization rate that we obtain ( $\Gamma_{-12} < 0.3s^{-1}$ ) is not enough to keep the IGM ionized and a substantial contribution to the UV background by faint AGNs is required. Since our sample is clearly still limited in size, larger  $z \sim 3$  LBG samples, at similar or even greater depths are necessary to confirm these results on a more firm statistical basis.

*Subject headings:* galaxies: distances and redshifts — Galaxies: evolution — Galaxies: high-redshift — intergalactic medium — diffuse radiation

## 1. Introduction

The evolution of the intergalactic medium (IGM) depends primarily on its ionization state, which at high redshifts is a function of the ionizing UV background (UVB) produced

by galaxies and AGNs. In the early universe, star forming (SF) galaxies are ubiquitous and in principle can provide the necessary flux to keep the IGM ionized at least up to  $z \sim 6$ , when the re-ionization appears to be completed (Fan et al. 2006). However, the poor knowledge of the average escape fraction of ionizing Lyman continuum photons from the interstellar medium of each galaxy introduces large uncertainties to the exact level of contribution in ionizing the IGM. The escape fraction of AGN is not strongly variable with redshift but the apparent number density of bright QSOs and AGNs is rapidly decreasing at  $z > 3$ , thus it is assumed that the contribution to the ionizing flux of the SF galaxies should become dominant at  $z > 3$  (e.g. Faucher-Giguère et al. 2008; Cowie et al. 2009). In this respect, several attempts have been made to derive the escape fraction of UV ionizing photons both at low redshifts, from space, and at high redshifts ( $z = 2-4$ ) from ground based observations. In most cases only upper limits on the escape fraction were obtained, giving little evidence to support a scenario where enough ionizing photons escape from galaxies. Actually, early measurements at low and intermediate redshifts, with  $f_{esc} \leq 1-3\%$ , seem to indicate that galaxies are not the major contributors to the ionizing UV background at  $z < 2$  leaving AGNs as the main ionizing population (e.g. Giallongo et al. 1997; Malkan et al. 2003; Siana et al. 2007; Cowie et al. 2010; Siana et al. 2010; Bridge et al. 2010).

At high redshifts direct observations of the Lyman continuum flux for galaxies at  $z > 4$  are difficult because of the sharp increase in the neutral hydrogen absorption by the IGM. For ground-based surveys, the search has thus been focused at  $z \sim 3 - 4$  which is a compromise between lower detection efficiency in the UV and higher transparency of the IGM in comparison to higher  $z$ . In this respect, there are two main strategies to face the issue of escaping ionizing photons from galaxies. One way is to derive direct constraints using very deep UV imaging and/or spectroscopic observations in order to ascertain if even a small fraction of LyC escapes from typical star forming galaxies. Such surveys are time consuming, requiring 20-30 hours of integration for reasonable UV efficiency, and for this reason involve small samples made up of some tens of galaxies. The works by Steidel et al. (2001) and Shapley et al. (2006) are typical in this respect. Indeed, Steidel et al. (2001) first claimed appreciable ionizing flux corresponding to a relative (with respect to the observed  $1500\text{\AA}$  flux) escape fraction of the order of  $> 50\%$  from a composite spectrum of the bluest 29 galaxies of their large LBG sample at  $z \sim 3.4$ . If such an escape fraction were typical of the LBG population, this would imply an ionizing UVB at least 3 times higher than the one derived from the analysis and modeling of the Lyman  $\alpha$  absorption by the IGM at the same redshift (e.g Bolton et al. 2005). Giallongo et al. (2002) obtained the first high S/N long slit spectra of two LBGs at  $z = 3$  and  $z = 3.3$ , selected from Steidel’s sample, where no significant Lyman continuum emission has been detected. This implies a  $1\sigma$  upper limit to the relative escape fraction of  $15\%$ . Using individual spectra of 14 LBG galaxies at  $z \sim 3$

Shapley et al. (2006) found significant emission only in two galaxies, implying a detected average relative escape fraction of 14% for their sample at a  $3\sigma$  confidence level, which is  $\sim 4.5$  times lower than the value derived by Steidel et al. (2001). The fact that the estimate of the escape fraction value obtained in this way has been progressively reducing from 70% to 15%, reveals the difficulties and the uncertainties involved in such measurements.

Another way to measure escaping ionizing flux is to use shallower UV imaging but of a very large sample of galaxies. In this case, instead of measuring the average/typical escape fraction of the population, the effort is concentrated in finding possible small fractions of special types of galaxies which could show a large percentage ( $>50\%$ ) of escaping ionizing flux. The main limitations of this method are the absence of extensive spectroscopic confirmation of the redshifts in the sample or, whenever spectral information is available, the large redshift range of the sources, which requires extended simulations to correctly account for the variances of IGM absorption, and the lower S/N level of the narrow band (NB) images. Typical in this direction is the work by Iwata et al. (2009), who have used a UV narrow band filter technique and found ionizing radiation, at a  $2\sigma$  level, in 7 out of 73 LBGs at  $z > 3$  LBGs and 10 out of 125 Ly $\alpha$  emitters at  $z > 3$  out of a sample of 198  $z > 3$  galaxies in the SSA22 field. The relative escape fraction derived for these 7 detected LBGs reaches 80%. It is interesting to note that they report null emission for the object SSA22a-D3, for which Shapley et al. (2006) claimed an ionizing flux detection. Moreover in several cases (including the second object detected by Shapley et al. 2006), an offset is present between the position of the object in the UV narrow band filter and in the R band detection image, suggesting possible contamination by interlopers. Vanzella et al. (2010b) evaluated the probable cause of such offsets, showing that there is a  $> 50\%$  probability for contamination, by lower  $z$  objects, in at least 30% of the galaxies showing clear Lyman continuum detection. Recently, Vanzella et al. (2010a) using ultra-deep VIMOS intermediate U band and deep FORS1 narrow band imaging of 102 galaxies in the GOODS-South at  $z \sim 3.7$ , obtained an  $f_{esc}$  upper limit of 5%-20% at a  $3\sigma$  level, depending on the assumed extinction curve and E(B-V) value, as well as the luminosity and redshift of the sources adopted in the analysis.

These two approaches should be considered as complementary, since they give us information on different aspects of the problem: the typical escape fraction from the majority of galaxies, the former, and the existence of rare galaxies with higher escape fractions, the latter. Both methods are necessary to measure with greater accuracy the global amount of ionizing flux in the universe. In the present paper we use deep U and R band imaging obtained by the UV optimized Large Binocular Camera (Giallongo et al. 2008) in two Steidel fields and in a region of the COSMOS field to derive stringent limits on the ionizing escape fraction of 11 LBGs at  $z \sim 3.3$ . The uniqueness of our data is represented by the simultaneous availability of very deep UV images, obtained with one of the most efficient ground based

large field UV imager at an 8m class telescope, in fields where spectroscopically confirmed galaxies in a very narrow redshift range around  $z \sim 3.3$ , are already available. This sample, although it is limited in size, gives us the possibility to focus on a very small redshift range, reducing appreciably the effect of the variation with redshift of the IGM opacity and allowing a more direct measure of the relative ionizing escape fraction from LBGs at  $z \sim 3.3$ .

## 2. Data

The targets were selected from three fields where deep UV images were obtained with the Large Binocular Camera (LBC) at the Large Binocular Telescope (LBT, Hill et al. 2010). The LBC has two channels, one optimized for the UV and blue bands and one optimized for imaging in the red bands, that was used to obtain the R band images. The detectors have four 4K×2K chips with a pixel scale of  $0.23 \text{ arcsec/pixel}$ , providing an unvignetted field of view of about  $23 \times 23 \text{ arcmin}^2$ . The standard LBC pipeline (Giallongo et al. 2008) has been used for data reduction. In particular, after creating the bias-subtracted images, we have applied standard flat-fielding using sky flats obtained during twilight. The sky background was subtracted using SExtractor (Bertin & Arnouts 1996) with a background mesh of  $64 \times 64$  pixels and adopting a median filter of  $3 \times 3$ . The astrometric solution was computed using the software AstromC developed by Radovich et al. (2004) and the USNO-A2 (Monet 1998) as reference catalog. After applying the astrometric correction, we have coadded the various images to create deep mosaics for each field. We did not include a color term in the photometric calibration and the accuracy of the zeropoint is 0.03-0.05 for the U filter. Part of these images have already been used to derive the number counts in the U band by Grazian et al. (2009) providing good agreement with previous results.

For each scientific image the LBC pipeline computes a corresponding RMS map directly from the raw science frames. We obtained the absolute RMS maps for each pointing by computing the RMS in each individual image (using Poisson statistics and the instrumental gain as  $\sigma_i = \sqrt{\frac{N_{ADU}}{\text{gain}}}$ ) and self-consistently propagating this RMS over the whole data reduction process. The delivered RMS maps were found to be consistent with the absolute RMS expected for each image and with the median RMS derived from  $5 \times 5$  pixel boxes in random positions of the sky (see Gawiser et al. (2006) for details).

Two LBC fields come from Steidel’s sample and include the bright quasars Q0933+28 ( $\alpha=09:33:31$ ,  $\delta=+28:44:42$ ) and Q1625+26 ( $\alpha=16:25:30$ ,  $\delta=+26:52:31$ ) (Steidel et al. 2003; Reddy et al. 2008). A major advantage that led to the selection of these areas is the existence of several spectroscopic redshifts, obtained by Steidel et al. (2003) in the redshift range  $2 < z < 3.5$ . The LBC images were obtained in the period 2007-2009 in the U band with

total exposure times of 12h and 8h, respectively, and in the R band with total exposure times of 2.8h and 3.4h. The AB magnitude limits reached at  $1\sigma$  in the U band are 28.8 and 28.6 and in the R band 25.5 and 25.9 at  $10\sigma$ , respectively, using an aperture of  $2\times\text{FWHM}$ . The seeing in the R band is  $1.0''$  for Q0933+28 and  $0.8''$  for Q1625+26. For both fields, the average seeing in the U band is  $1.1''$ .

The third LBC field is within the COSMOS field (Scoville et al. 2007; Lilly et al. 2007) where extensive multiband and spectroscopic dataset is continuously improving. The LBC observations of the COSMOS field started in February 2007 to add deep UGRIZ imaging in the central  $1\text{ deg}^2$  and are currently on-going. The exposure time per pointing in the U band is  $\sim 6$  hours, for a total of three partially overlapping LBC pointings, reaching 11 hours at the deepest region. Actually, the whole area covered by deep *UGRIZ* data in COSMOS is  $\sim 700$  sq. arcmin. and reaches a  $1\sigma$  AB magnitude limit of  $U=28.7$ , with a typical seeing of  $1.0''$ . The R band image has an average seeing of  $0.9''$  and it reaches an AB magnitude limit of  $R=25.9$  at  $10\sigma$ , for two pointings. The third pointing was obtained during commissioning and it has a total exposure time of 0.5 hours, an average seeing of  $0.9''$  and an AB magnitude limit of  $R=23.8$ . The datasets in all three fields are composed by different mosaics, obtained in different years and in a variety of seeing conditions and exposure times. Although we have average seeing values estimated in each band, these values do not remain stable throughout the whole final mosaic. Actually, the seeing in the R band ranges from  $0.8''$  to  $1.0''$  and in the U band from  $1.0''$  to  $1.2''$ , especially in the COSMOS field where we cover the largest area and we have 3 different pointings with different final exposure times.

### 3. Analysis

It is important to note that there are several definitions for the ionizing escape fraction which depend on the non-ionizing flux considered as a reference. The absolute escape fraction is the ratio between the escaping Lyman continuum flux and the one intrinsically produced by stars in the galaxy (Leitherer et al. 1995). In practice this value is difficult to determine because we should know the intrinsic Lyman continuum flux from an accurate fit to the overall spectral energy distribution of the galaxy. For this reason, observationally, the ionizing escape fraction is usually related to the rest frame  $1500\text{\AA}$  flux and denoted as  $f_{esc}$ . This reference flux is however attenuated by dust and a correction is needed if we want to derive the intrinsic Lyman continuum. If the amount of dust attenuation is not known in the analyzed galaxy sample, a relative escape fraction  $f_{esc}^{rel}$  can be introduced as the fraction of escaping Lyman continuum photons divided by the fraction of escaping photons at  $1500\text{\AA}$  (Steidel et al. 2001). The relation between the two quantities is  $f_{esc} = f_{esc}^{rel} \times 10^{-0.4A_{1500}}$

where  $A_{1500}$  is the dust absorption at  $1500\text{\AA}$  (Inoue et al. 2006; Vanzella et al. 2010a). Since LBGs at  $z=3$  show an average  $A_{1500}=0.6$  (Vanzella et al. 2010a) then  $f_{esc}^{rel}$  should be typically 2 times larger than  $f_{esc}$ . Finally, to derive the Lyman continuum ionizing fraction from the observed fluxes at  $900\text{\AA}$  and  $1500\text{\AA}$ , we need to estimate the contribution to the absorption by the intervening IGM and the average intrinsic UV spectral shape of the galaxy populations. In our analysis we estimated the relative escape fraction using the following equation:

$$f_{esc}^{rel} = \frac{(L_{1500}/L_{900})_{int}}{(f_{1500}/f_{900})_{obs}} \exp(\tau_{900}^{IGM}) \quad (1)$$

where  $(L_{1500}/L_{900})_{int}$  is the average intrinsic ratio of non-ionizing to ionizing specific intensities as derived from spectral synthesis models (e.g. Bruzual & Charlot 2003),  $(f_{1500}/f_{900})_{obs}$  is the observed flux ratio estimated from our U-R color and  $\exp(\tau_{900}^{IGM})$  is the inverse of the average IGM transmission at  $z \sim 3.3$ . For comparison with previous estimates of  $f_{esc}^{rel}$  in the literature, we adopt  $(L_{1500}/L_{900})_{int}=3$ , but this value is model dependent and will be discussed below. A major issue in the derivation of the relative escape fraction is the estimate of the average attenuation produced by the IGM along the line of sight,  $\exp(\tau_{900}^{IGM})$ . This value is very sensitive to the actual redshift distribution of the sources and to the wavelength bandpass of the filters used. The broader the filter, the more the luminosity of the continuum at  $\lambda \leq 912\text{\AA}$  will be diluted, resulting to a less constraining value for the escape fraction.

The average IGM transmission  $\exp(-\tau_{900}^{IGM})$  for our galaxy sample has been derived following the work of Prochaska et al. (2009), where they analyzed the average rest-frame spectra of  $z>3$  SDSS quasars. They measured the IGM absorption from the drop of the flux at  $\lambda \leq 912\text{\AA}$ , rest frame, in a redshift range  $3.6 < z < 4.3$ . To reproduce the IGM attenuation at  $z \sim 3.3$ , instead of using the Lyman absorption statistical distribution in column density and redshift, we decided to adopt the same empirical fit described by the authors. More specifically, since the lowest redshift they consider is 3.6, we extrapolated the IGM LyC absorption to the average redshift of our sample ( $z=3.3$ ) using the formula (Eq.6) given by Prochaska et al. (2009), and adding the contribution of the Lyman series absorption using the equations described by Fan et al. (2006). The attenuation of photons that were emitted at an observed wavelength,  $\lambda_{obs}$ , at redshift  $z_{em}=3.3$ , is shown in Fig. 1 (solid black line).

The LBC UV broad band transmission covers the wavelength range from  $3200\text{-}3900\text{\AA}$ , with a small tail up to  $4000\text{\AA}$  (considering an average airmass for our dataset of 1.2 and including instrument and CCD response). This means that Lyman continuum emission by LBGs at  $\lambda < 912\text{\AA}$  starts just short-wards of the red edge of the U filter for sources with  $z \simeq 3.3$ , leaving the LBGs non ionizing emission outside the filter at  $\lambda_{obs} > 4000\text{\AA}$ . The

effective rest-frame wavelength for the Prochaska IGM attenuation, convolved with the LBC U band filter and considering  $z=3.3$ , is  $860\text{\AA}$ , which is reasonably close to  $900\text{\AA}$ . Thus, in order to avoid contamination from continuum emission red-wards of the Lyman limit and to probe a wavelength close to  $900\text{\AA}$ , without introducing excessive dilution of the observed emission due to IGM attenuation, we decide to use only LBGs with spectroscopic redshifts in the range  $3.27 < z < 3.35$ . We consider this as the best trade-off in order to obtain tight constraints for the escape fraction.

We have a total of 12 LBGs in the tight redshift range ( $3.27 < z < 3.35$ ) in all of our fields: 4 sources in Q0933, 1 in Q1623 and 7 in COSMOS. In the COSMOS field one of the sources ( $\alpha=10:01:19.29$ ,  $\delta=+02:04:20.2$ ) showed significant emission in the U band ( $> 3\sigma$ ), which was slightly offset from the image center in the R band. We checked the high resolution ACS image finding that the morphology of the source appears more consistent with two distinct objects, which are too close to be resolved in ground based observations. Careful inspection of the spectrum also supports such a scenario, where the main spectral features clearly appear only in the UV dropout candidate. In the LBC images there is an offset of  $\sim 0.6''$ , between the emission in the R and U band that corresponds to  $\sim 6\text{kpc}$ . For all these reasons, we decided not to include this source in our sample, leaving us with a total of 11 LBGs in the 3 fields. According to Vanzella et al. (2010b), assuming the number counts for  $U < 28.5$  with a seeing of  $1''$ , there is more than 80% probability that 10% of the sources are affected by contamination from lower redshift sources in the line of sight. Thus, the fact that 1 out of our 12 LBGs seems to be contaminated is within the statistical limits.

To compute a reliable upper limit to the Lyman continuum escape fraction we created thumbnail images of  $45'' \times 45''$  in the U and R bands around each of the selected sources. The size of the thumbnail is large enough to obtain a reliable estimate for the background, which is subtracted after masking the surrounding objects. We then sum all thumbnails in each band creating a stacked image, where the flux corresponds to the weighted mean value of the fluxes of the individual images in each band. In Fig. 2 we show the result of this procedure. We obtained aperture photometry around the source in the R band ( $f_{1500}$ ) where the source is visible, extracting the center of the stacked profile. This position is then used to measure the expected aperture flux in the U band image ( $f_{900}$ ). Fig. 2 shows no significant flux in the U band stacking. In order to establish the optimum apertures for the photometry we created a stacking of stars. The selected stars are near our candidates in the 3 fields, and their flux has been normalized in order to get the same magnitude distribution of the LBG stacking. This is necessary since the magnitudes of the LBGs used vary significantly and the characteristics of the brightest sources will be more prominent in the final stack. The average measured stellar FWHM is  $0.9''$  in the R and  $1.1''$  in the U band. Using the stellar PSF, we have created a kernel that matches the PSF in the R band to the one in

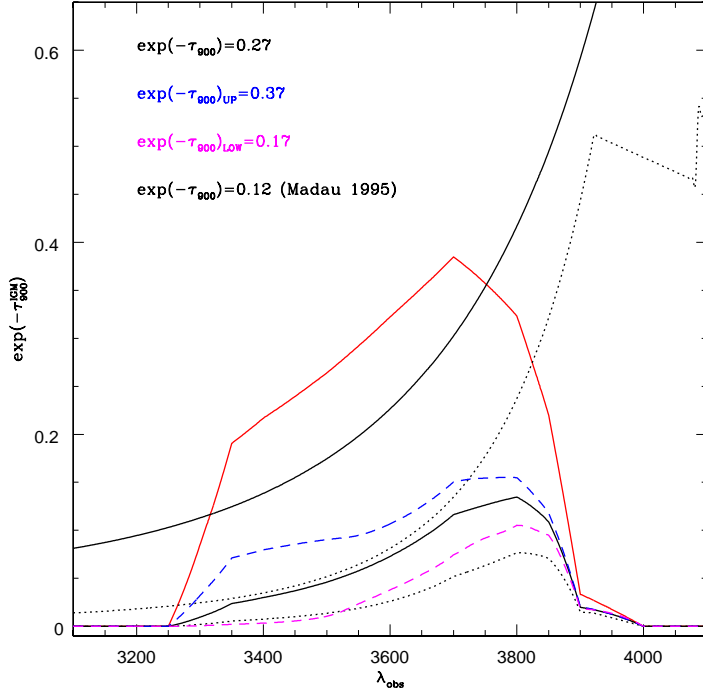


Fig. 1.— The IGM transmission is calculated using the Prochaska et al. (2009) value extrapolated at  $z=3.3$  (black solid line) along with the total transmission curve for our U band (red solid line). The lower black dotted line corresponds to the Madau IGM transmission and it is shown for comparison only. The solid and dotted lines under the filter transmission are the resulting  $\exp(-\tau_{900}^{IGM})$  curves after the convolution with the filter response using the Prochaska and Madau IGM transmission curves respectively. The color-coded lines correspond to the upper and lower limit of the IGM attenuation showing the uncertainty in our measurement as given by the work of Prochaska et al. (2009) (see parag. 4 for details). The filter transmission and the resulting  $\exp(-\tau_{900}^{IGM})$  curves after the convolution have all been multiplied by a factor of 2 to facilitate the view. At  $\lambda \approx 3700$  the real filter transmission value is 0.19.



the U band. Once calculated, such Gaussian filter has been applied to the R band image of the LBG stacking, in order to match the R band morphology to the expected U band size. The finally adopted aperture diameters correspond to  $1.5 \times \text{FWHM}$  in U band, namely, 7.3 pixels. The magnitude measured in the smoothed R band is 24.35 mag (AB). The  $1\sigma$  rms background error in the U band has been used as the flux upper limit and it is equivalent to a lower limit in magnitude of  $U \geq 30.7(AB)$  at  $1\sigma$  confidence level for the LBG stacking.

#### 4. Results and Discussion

Using the 11 sources with spectroscopic redshift  $z \sim 3.3$  we obtain  $(f_{1500}/f_{900})_{obs} \geq 224$ . Considering the average IGM attenuation extrapolated at this redshift from the Prochaska value ( $\exp(-\tau_{900}^{IGM})=0.27$ ), we derive  $f_{esc}^{rel} \leq 0.05$  (5%) at  $1\sigma$ . Compared to the values in the literature so far, this is one of the most constraining results for this redshift range. An additional advantage of our sample is that it covers 3 independent areas in the sky and includes spectroscopically confirmed LBGs that have been selected through different methods. More specifically, the LBGs in the Q0933 field are U drop-out sources, the one in the Q1623 field is a BX candidate (Reddy et al. 2008) and out of the 6 sources in COSMOS, 4 have been selected as both U drop-out and gzK candidates, while 2 are only U drop-out candidates.

For a more detailed approach, we used the same technique to estimate the escape fraction also for individual sources. The resulting values are presented in Table 1. The average magnitude of the sources is  $\sim 24.4$  in the R band and the values of the upper limits of the relative escape fraction for individual sources range from  $<6\%$  to  $<36\%$ , with an average value of  $<21\%$ . To exclude the possibility that our result is biased by the wide range in

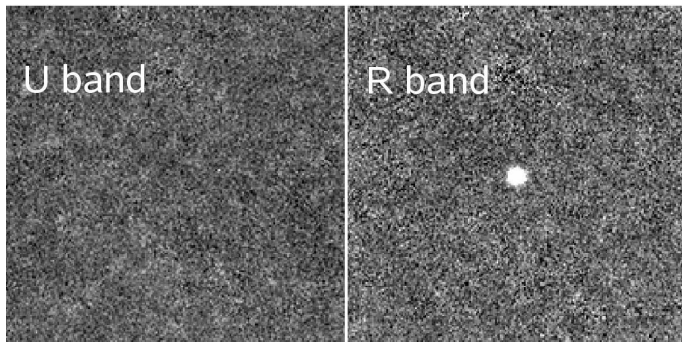


Fig. 2.— The stacking result for the 11 LBGs of our sample. The size of each thumbnail is  $45'' \times 45''$

the R magnitude we created a subset of our sample, where we used for the stacked image only the sources with  $23.5 < R < 24.7$  (6 sources). In this case we obtain a relative escape fraction of  $< 6\%$ .

As already stated in the introduction, there are two main uncertainties involved in the measurement of an accurate escape fraction, concerning the transmission of the IGM and the intrinsic  $L_{1500}/L_{900}$  ratio. The uncertainty associated to the IGM is computed following the work of Prochaska et al. (2009). Using the  $1\sigma$  limits they state for the IGM attenuation, we compute upper and lower limits for the value of  $\exp(\tau_{900}^{IGM})$ . This way, we obtain  $\exp(-\tau_{900}^{IGM})_{upper}=0.37$  and  $\exp(-\tau_{900}^{IGM})_{lower}=0.17$ , from which we derive  $(f_{esc}^{rel})_{lower} \leq 0.04$  (4%) and  $(f_{esc}^{rel})_{upper} \leq 0.08$  (8%) respectively. For comparison with early results in the literature we derive also the relative escape fraction using the Madau model. As seen in Fig.1 the  $\exp(-\tau_{900}^{IGM})_{Madau}$  is 0.12 and we obtain  $f_{esc}^{rel} \leq 0.11$  (11%). Since Madau’s first analysis, the statistics of IGM absorption have changed appreciably (e.g Fan et al. 2006; Meiksin 2006; Inoue & Iwata 2008) and Madau’s model represents now a lower limit to  $\exp(-\tau_{900}^{IGM})$  (Inoue & Iwata 2008), making the  $f_{esc}^{rel}$  value based on this model an upper bound. In fact, considering all uncertainties we find that the highest upper limit for the escape fraction in no case exceeds 11%, that corresponds to twice our fiducial value.

Another source of uncertainty in estimating the relative escape fraction is the assumed value for the parameter  $L_{1500}/L_{900}$ . So far, the most widely used value is  $L_{1500}/L_{900}=3$  (e.g. Steidel et al. 2001; Inoue et al. 2005; Shapley et al. 2006) and we have adopted it in order to facilitate the comparison of our results with previous works in the literature. Such value is derived considering typical models of UV SED for star-forming galaxies with constant star formation rate (SFR). However, this ratio of the intrinsic luminosities depends also on the age of the galaxy and on its star formation history (SFH). Even for constant SFH, Inoue et al. (2005) find that the intrinsic ratio depends on the time passed since the onset of star formation and ranges from 1.5 to 5.5, approaching the upper edge for older ages. More specifically Meiksin (2009) has found a  $f_{\nu}(1500\text{\AA})/f_{\nu}(912\text{\AA})$  that ranges from 2.7 considering 1Myr starbursts to 6.2-6.7 for 100-300Myr that are the typical ages of LBGs. If we consider an intrinsic luminosity ratio of 7, that is the value recently used by Vanzella et al. (2010a), our estimated escape fraction would increase by a factor of 2.3 ( $f_{esc}^{rel} \leq 11.5\%$ ).

Nevertheless, assessing the role of LBGs in producing the ionizing UVB does not depend on the assumed value for the parameter  $L_{1500}/L_{900}$ . Following the work by Inoue et al. (2006), where they define the Lyman continuum to UV escape flux density ratio, the luminosity density  $\rho_{900,esc}$  corresponds to:

$$\rho_{900,esc} = \rho_{1500} \frac{L_{900}}{L_{1500}} f_{esc}^{rel} = \rho_{1500} \left( \frac{f_{900}}{f_{1500}} \right)_{obs} \exp(\tau_{900}^{IGM}) \quad (2)$$

After converting the luminosity density uncorrected for dust extinction derived by Reddy & Steidel (2009) at  $1700\text{\AA}$  to  $1500\text{\AA}$ , we obtain  $\rho_{1500} = (3.61 \pm 0.24) \times 10^{26} \text{ergs}^{-1} \text{Hz}^{-1} \text{Mpc}^{-3}$ , which corresponds to a  $\rho_{900,esc} = 5.98 \times 10^{24} \text{ergs}^{-1} \text{Hz}^{-1} \text{Mpc}^{-3}$ . We note that this luminosity density has been obtained using the slope of the luminosity function (LF) given by Reddy & Steidel (2009),  $\alpha = -1.73 \pm 0.13$ , and integrating this LF down to their faint magnitude limit ( $M_{AB}(1500) = -17.6$  corresponding to  $R \sim 28$ ), assuming that the  $f_{esc}$  does not evolve with luminosity. If we consider sources with  $R \leq 25.5$ , that is the magnitude limit of our sample ( $M_{AB}(1500) = -20.2$ ), we obtain  $\rho_{1500} = 1.27 \times 10^{26} \text{ergs}^{-1} \text{Hz}^{-1} \text{Mpc}^{-3}$ , from which we derive  $\rho_{900,esc} = 2.1 \times 10^{24} \text{ergs}^{-1} \text{Hz}^{-1} \text{Mpc}^{-3}$ . At  $z \sim 3$  Bolton et al. (2005), using high resolution simulations to model the Ly $\alpha$  forest opacity, estimate the hydrogen ionization rate of the IGM as  $\Gamma_{-12} = 0.86_{-0.26}^{+0.34} s^{-1}$  (ionization rate in  $10^{-12} s^{-1} \text{atom}^{-1}$ ), which corresponds to a luminosity density of  $\rho_{900} = 16.5 \times 10^{24} \text{ergs}^{-1} \text{Hz}^{-1} \text{Mpc}^{-3}$ . The values presented by Bolton et al. (2005) are in good agreement with more recent works (e.g. Dall’Aglio et al. 2009). Our estimated contribution, derived from  $M_{AB}(1500) < -20$  sources, is significantly lower than the theoretical value. Even considering the contribution of fainter galaxies, the estimated emissivity does not increase enough in order to supply the required ionizing radiation. Due to our tight constraint on the escape fraction, we derive an upper limit to the hydrogen ionization rate  $\Gamma_{-12} < 0.3 s^{-1}$ , using as an average spectral index  $\alpha_{UV} = 1.8$  (Faucher-Giguère et al. 2008) and  $M_{AB}(1500) \leq -17.6$ . This is lower than the values reported by Bolton et al. (2005) and only including their estimated AGN contribution at  $z \sim 3$  ( $\Gamma_{-12} = 0.4 s^{-1}$ ), the ionization rate is barely consistent with the theoretical expectations from the Ly $\alpha$  forest analysis.

Here we should discuss the possibility of a bimodal distribution of the LyC escape fraction, where a small fraction of the galaxy population at a given redshift can be the major contributor to the cosmological ionizing flux. At present, our sample of 11 LBGs is still statistically modest and cannot exclude in a conclusive way the existence of a limited sub-group of galaxies with significant escape fraction. Moreover, the search for such rare strong LyC emitters at high redshifts is not as straightforward as at lower redshifts. Indeed, Cowie et al. (2009) found only 1 galaxy out of 600 presenting a significant fraction of escaping ionizing flux at  $z \sim 1$ . At higher redshifts, Iwata et al. (2009) claims that up to  $\sim 10\%$  of galaxies at  $z \sim 3.1$  show escape fractions at the level of  $\sim 80\%$ . However, an offset ( $1'' - 2''$ ) between the image in the R band, sampling the non-ionizing flux at  $\sim 1500\text{\AA}$  and the UV images, sampling the LyC flux, has been noted by the same authors. Since the escape fraction derived by the UV-R color in the detected LyC emitters is at a the level of  $\sim 80\%$ , this would imply an unrealistic fraction,  $> 100\%$ , from the limited spatial region where the claimed LyC emission is observed. Through statistical analysis, this number has been questioned by Vanzella et al. (2010b), claiming that at least 30% of those galaxies have more

than 50% probability of being low redshift interlopers. On the other hand, Vanzella et al. (2010a) have found only 1 galaxy out of 102 LBGs at  $3.4 < z < 4.5$  that shows strong LyC emission. In any case, assuming a population of strong LyC emitters were present at  $z=3$ , this could be at most of the order of 1-7% for the overall population. Adopting this contamination fraction as a reference value, the contribution of this subsample to the UV emissivity translates to an increase in the ionization rate of the order of  $\Gamma_{-12}=0.1-0.3s^{-1}$ , to be added to our original upper limit ( $\Gamma_{-12} < 0.3s^{-1}$ ). Even in this case, the ionization rate is still not sufficient to keep the IGM ionized, making necessary an appreciable contribution by some other population, possibly AGN or a large number of very faint star forming galaxies with increasingly larger escape fractions.

Such a scenario, where the AGN contribution is still important at  $z > 3$  is also supported by the work of Siana et al. (2008), who derive an ionization rate of  $\Gamma_{-12} = 0.48s^{-1}$  for QSOs at  $z \sim 3.2$ , suggesting that AGN and LBGs are emitting comparable fractions of ionizing flux to the intergalactic medium. This is in agreement with recent results by Glikman et al. (2011), who find that the AGN account for at least half the ionizing radiation needed at these redshifts ( $60\pm 40\%$ ). Moreover, our observed limit for the  $f_{esc}^{rel}$ , is closer to the values reported by large surveys at lower redshifts ( $1 < z < 2$ ) suggesting a milder evolution with redshift. Deeper UV and narrow band observations of larger statistical samples of LBGs at  $z\sim 3$  will allow us to clarify this issue.

K.B. would like to thank N. Reddy for providing redshifts for the sources in the Steidel fields. Observations have been carried out using the Large Binocular Telescope at Mt. Graham, Arizona. The LBT is an international collaboration among institutions in the United States, Italy and Germany. LBT Corporation partners are: The University of Arizona on behalf of the Arizona university system; Istituto Nazionale di Astrofisica, Italy; LBT Beteiligungsgesellschaft, Germany, representing the Max-Planck Society, the Astrophysical Institute Potsdam, and Heidelberg University; The Ohio State University, and The Research Corporation, on behalf of The University of Notre Dame, University of Minnesota and University of Virginia.

## REFERENCES

- Bolton, J. S., Haehnelt, M. G., Viel, M., & Springel, V. 2005, MNRAS, 357, 1178
- Bertin, E., & Arnouts, S. 1996, A&AS, 117, 393
- Bridge, C. R., Teplitz, H. I., Siana, B., et al. 2010, ApJ, 720, 465

- Bruzual, G., & Charlot, S. 2003, MNRAS, 344, 1000
- Chen, H.-W., Prochaska, J. X., & Gnedin, N. Y. 2007, ApJ, 667, 125
- Cowie, L. L., Barger, A. J., & Hu, E. M. 2010, ApJ, 711, 928
- Cowie, L. L., Barger, A. J., & Trouille, L. 2009, ApJ, 692, 1476
- Dall’Aglio, A., Wisotzki, L., & Worseck, G. 2009, arXiv:0906.1484
- Fan, X., Strauss, M. A., Becker, R. H., et al. 2006, AJ, 132, 117
- Faucher-Giguère, C.A., Lidz, A., Hernquist, L., & Zaldarriaga, M. 2008, ApJ, 688, 85
- Fernández-Soto, A., Lanzetta, K. M., & Chen, H. 2003, MNRAS, 342, 1215
- Fynbo, J. P. U., Jakobsson, P., Prochaska, J. X. et al. 2009, ApJS, 185, 526
- Gawiser, E., van Dokkum, P. G., Herrera, D. et al. 2006, ApJS, 162, 1
- Giallongo, E., Ragazzoni, R., Grazian, A., et al. 2008, A&A, 482, 349
- Giallongo, E., Cristiani, S., D’Odorico, S., & Fontana, A. 2002, ApJ, 568, 9
- Giallongo, E., Fontana, A., & Madau, P. 1997, MNRAS, 289, 629
- Glikman, E., Djorgovski, S. G., Stern, D., et al. 2011, ApJ, 728, 26
- Grazian, A., Menci, N., Giallongo, E., et al. 2009, A&A, 505, 1041
- Hill, J. M., Green, R. F., Ashby, D. S., et al 2010, SPIE, 7733, 10
- Inoue, A. K. & Iwata, I. 2008, MNRAS, 387, 1681
- Inoue, A. K., Iwata, I., & Deharveng, J. 2006, MNRAS, 371, 1
- Inoue, A. K., Iwata, I., Deharveng, J., Buat, V., & Burgarella, D. 2005, A&A, 435, 471
- Iwata, I., Inoue, A. K., Matsuda, Y., et al. 2009, ApJ, 692, 1287
- Leitherer, C., Ferguson, H. C., Heckman, T. M., & Lowenthal, J. D. 1995, ApJ, 454, 19
- Leitherer, C., Schaerer, D., Goldader, J. D. et al. 1999, ApJS, 123, 3
- Lilly, S. J., Le Fèvre, O., Renzini, A., et al. 2007, ApJS, 172, 70
- Madau, P. 1995, ApJ, 441, 18

- Malkan, M., Webb, W., & Konopacky, Q. 2003, *ApJ*, 598, 878
- Meiksin, A. 2006, *MNRAS*, 365, 807
- Meiksin, A. 2009, *RvMP*, 81, 1405
- Monet, D. G., 1998, *A&AS*, 19312003
- Prochaska, J. X., O’Meara, J. M., & Worseck, G. 2010, *ApJ*, 718, 392
- Prochaska, J. X., Worseck, G., & O’Meara, J. M. 2009, *ApJL*, 705, 113
- Radovich, M., Arnaboldi, M., Ripepi, V. et al. 2004, *A&A*, 417, 51
- Reddy, N. A. & Steidel, C. C. 2009, *ApJ*, 692, 778
- Reddy, N. A., Steidel, C. C., Pettini, M., et al. 2008, *ApJS*, 175, 48
- Scoville, N., Aussel, H., Brusa, M., et al. 2007, *ApJS*, 172, 1
- Shapley, A. E., Steidel, C. C., Pettini, M. et al. 2006, *ApJ*, 651, 688
- Siana, B., Teplitz, H. I., Colbert, J., et al. 2007, *ApJ*, 668, 62
- Siana, B., Polletta, M. d. C., Smith, H. E., et al. 2008, *ApJ*, 675, 49
- Siana, B., Teplitz, H. I., Ferguson, H. C., et al. 2010, *ApJ*, 723, 241
- Songaila, A. & Cowie, L. L. 2010, *ApJ*, 721, 1448
- Steidel, C. C., Adelberger, K. L., Shapley, A. E., et al. 2003, *ApJ*, 592, 728
- Steidel, C. C., Pettini, M., & Adelberger, K. L. 2001, *ApJ*, 546, 665
- Vanzella, E., Giavalisco, M., Inoue, A., et al. 2010a, *ApJ*, 725, 1011
- Vanzella, E., Siana, B., Cristiani, S., & Nonino, M. 2010b, *MNRAS*, 404, 1672

Table 1: Summary of the  $f_{esc}^{rel}$  values for the individual LBGs.

| ID    | RA        | DEC       | $z$  | Rmag<br>$\pm 0.07$ | Umag<br>$1\sigma$ (u.l) | $f_{esc}^{rel}$<br>$1\sigma$ (u.l) |
|-------|-----------|-----------|------|--------------------|-------------------------|------------------------------------|
| 3400  | 143.35424 | +28.80694 | 3.27 | 24.88              | 29.75                   | 0.203                              |
| 12646 | 143.32868 | +28.71913 | 3.33 | 25.13              | 29.61                   | 0.329                              |
| 8556  | 143.38236 | +28.75308 | 3.33 | 24.91              | 29.66                   | 0.258                              |
| 10849 | 143.36004 | +28.73414 | 3.35 | 25.59              | 29.66                   | 0.357                              |
| 17175 | 246.46910 | +26.89244 | 3.34 | 24.69              | 29.05                   | 0.235                              |
| 74113 | 149.88620 | +2.276064 | 3.33 | 23.56              | 29.66                   | 0.062                              |
| 50989 | 149.83421 | +2.416729 | 3.31 | 24.61              | 29.25                   | 0.223                              |
| 32388 | 149.77887 | +2.229502 | 3.30 | 24.63              | 29.60                   | 0.163                              |
| 51227 | 149.89208 | +2.414816 | 3.28 | 24.45              | 29.28                   | 0.202                              |
| 1723  | 150.44702 | +2.347633 | 3.30 | 23.63              | 28.23                   | 0.234                              |
| 13903 | 150.41495 | +2.158999 | 3.29 | 22.59              | 28.79                   | 0.056                              |
| stack | –         | –         | 3.3  | 24.85              | 30.73                   | 0.050                              |